

# Engineered collagen-binding bone morphogenetic protein-2 incorporated with platelet-rich plasma accelerates lumbar fusion in aged rats with osteopenia

Weiguo Zhu<sup>1,2</sup> , Chao Kong<sup>1,2</sup>, Fumin Pan<sup>1,2</sup>, Miao Ouyang<sup>1,2</sup>, Kang Sun<sup>1,2</sup> and Shibao Lu<sup>1,2</sup>

<sup>1</sup>Department of Orthopaedic Surgery, Xuanwu Hospital of Capital University of Medical Sciences, Beijing 100053, China; <sup>2</sup>National Clinical Research Center for Geriatric Diseases, Beijing 100053, China

Corresponding author: Shibao Lu. Email: spinelu@163.com

## Impact statement

In aged individuals, osteopenia is a great concern for achieving solid spinal fusion. Spinal malunion could lead to various implant-related complications and reduce postoperative quality of life. Most previous authors performed studies concerning osteoinductive strategy in young animal models whose osteopenia was induced by physical or chemical methods. Based on the physiological characteristics of osteogenic and angiogenic dysfunction in aging body, this study first uses an effective sustained delivery system of collagen scaffold binding with bone morphogenetic protein-2 (CBD-BMP-2) to enforce the spinal fusion in aged rats with osteopenia and explores whether platelet-rich plasma (PRP) could help CBD-BMP-2 to achieve a better outcome in terms of bone repair. Our approving results could provide a reference for clinical practice to address the postoperative complications associated with osteopenia in elderly patients.

## Abstract

In aged individuals, osteopenia is a great concern for achieving solid spinal fusion. Spinal malunion could lead to various implant-related complications and reduce postoperative quality of life. This study aims to investigate the efficacy of collagen-binding bone morphogenetic protein-2 (CBD-BMP-2) on the treatment of lumbar inter-transverse defects and to explore whether platelet-rich plasma could help CBD-BMP-2 to achieve a better outcome in terms of osteogenesis in senile rats with osteopenia. *In vitro* experiment proved the angiogenic function of platelet-rich plasma and osteogenic effect of CBD-BMP-2. Rats were performed posterolateral lumbar inter-transverse fusion. Rats implanted with CBD-BMP-2 + platelet-rich plasma were assigned to Group A ( $n=20$ ), rats implanted with CBD-BMP-2 were assigned to Group B ( $n=20$ ), and those with platelet-rich plasma were assigned to Group C ( $n=20$ ). Four weeks after implantation, radiographic assessment, manual palpation, and histological evaluation were performed. *In vivo* experiments showed satisfactory therapeutic effect on lumbar inter-transverse fusion in both Groups A and B and better results of bone microarchitecture in Group A. Solid fusion rate was 77.8% in Group A, 66.7% in Group B, and 0% in Group C ( $P < 0.001$ ). Our study indicated that CBD-BMP-2 could effectively facilitate the lumbar inter-transverse fusion in aged rats with osteopenia and platelet-rich plasma could help CBD-BMP-2 to enhance the bone healing of vertebral defects.

**Keywords:** Osteopenia, bone morphogenetic protein-2, collagen-binding, sustained release, platelet-rich plasma, spinal fusion

*Experimental Biology and Medicine* 2021; 246: 1577–1585. DOI: 10.1177/15353702211001039

## Introduction

Entering the aging society, more and more elderly patients suffering from degenerative spinal disorders receive spinal fusion surgeries to improve their living qualities. For these individuals, osteoporosis is a great concern for achieving solid spinal fusions and satisfactory long-term outcomes.<sup>1,2</sup> Primarily attributed to the dysfunctions of bone marrow mesenchymal stem cells (BMSCs) and osteoblasts, osteoporosis is generally characterized by osteopenia and microarchitecture deformation.<sup>3</sup> Management of osteoporotic bone defect is often hindered by reduced bone healing, subsequent disability, and increased complications.<sup>4,5</sup>

Promoting osteoblast activity with the help of biological agents is a feasible approach to prevent the nonunion-related problems, in addition to improving surgical techniques.<sup>6,7</sup> As the most effective osteoinductive factor, bone morphogenetic protein-2 (BMP-2) has gradually become the focus of laboratory and clinical researches.<sup>8,9</sup> A great deal of bone defect models has verified its effectiveness on increasing bone cell proliferation and promoting bone regeneration. In most cases, however, BMP-2 was delivered through physical or electrostatic adsorption without strong binding affinity to scaffold. Releasing BMP-2 in burst would result in quick degradation upon initial

implantation and restrict its therapeutic effect on bone repair in a prolonged period.<sup>10,11</sup>

In order to address this problem, a collagen-binding domain (CBD) was introduced to tightly bind BMP-2 to the collagen scaffold (CBD-BMP-2), which could maintain BMP-2 at high local concentration and prolong its bioavailability.<sup>12,13</sup> With good biocompatibility and bioactivity, this recombinant collagen-binding factor CBD-BMP-2 has been demonstrated to be able to effectively improve the bone healing in several animal models with better histological and radiographic results, indicating its promising prospect of application and spreading.<sup>8,14-16</sup> In a recent study, Cui *et al.*<sup>16</sup> used CBD-BMP-2 to help bovine bone collagen particle (BBCP) to promote bone repair in vertebral laminar defect model in the newly weaned rabbits. Laminar defects recovered better in BBCP/CBD-BMP-2 group than BBCP group. They concluded that BBCP combined with CBD-BMP-2 might be a good strategy for vertebral laminar defects in children. Up to now, however, the efficiency of this bone repair system on promoting bone healing is still unknown in the aging body with osteopenia.

Concerning the physiological characteristic of slow bone metabolism, biological agents are more necessary in aging body. Besides the dysfunctions of bone cells, bone microcirculatory disturbance was also described in the senile animals with osteoporosis,<sup>17-19</sup> which would restrict the bone homeostasis and repair.<sup>20</sup> Authors even found dysfunctional microcirculation of lumbar vertebral marrow might be prior to bone loss.<sup>21</sup> As a highly concentrated form of autogenous platelets, platelet-rich plasma (PRP) contains a rich source of angiogenic and osteogenic factors that play an important role in angiogenesis and osteogenesis.<sup>22,23</sup> Therefore, we designed the present study to investigate the efficacy of CBD-BMP-2 in the treatment of lumbar inter-transverse defects and to explore whether PRP could help CBD-BMP-2 to achieve a better outcome in terms of osteogenesis in senile rats with osteopenia.

## Materials and methods

### Aged osteopenia rats

The study protocol was approved by the Ethics Committee of Xuanwu Hospital of Capital University of Medical Sciences. Senile male Sprague Dawley rats aged 18 month and young rats aged 8 week were purchased from Beijing Vital River Laboratory Animal Technology Co., Ltd (Beijing, China). Ten senile rats and 10 young rats were sacrificed to test the bone mineral density (BMD) of their isolated lumbar vertebrae, using dual-energy X-ray absorptiometry (NORLAND XR-46, USA).<sup>24</sup> Senile rats were confirmed to have reduced BMD relative to younger rats.

### Preparation of demineralized bone matrix scaffolds

Demineralized bone matrix (DBM) that was mainly composed with collagen was produced from bovine's spongy bone as previously described.<sup>13,25</sup> Spongy bones were separated and cut into proper size, followed by soaked in acetone for 48 h to remove the fatty composition. After washed by ddH<sub>2</sub>O, enzyme treated and washed again by ddH<sub>2</sub>O,

the spongy bones were demineralized using the 0.6 M HCl and then freeze-dried.

### CBD-BMP-2 preparation

The preparation of CBD-BMP-2 was followed by the previous procedures.<sup>8</sup> The DNA sequence of hexahistidine and DNA fragment of mature human BMP-2 were inserted into bacterial expression vector pET-28a (Novagen, Germany), followed by transformed into BL21 strain of *E. coli*. The fusion protein was then induced by 1 mM isopropylthiogalactopyranoside to express recombinant protein. The target protein was separated as inclusion body from the lysate of *E. coli*, collected by centrifugation, and purified with chromatography. After renatured, the fusion protein CBD-BMP-2 was concentrated by ultrafiltration.

### Preparation of PRP<sup>26</sup>

Ten male rats aged 18 month were selected as donors for PRP preparation. Blood samples taken from the right ventricle were transferred into test tubes that contained 3.2% sodium citrate (blood/citrate ratio was 9:1), followed by centrifugation at 400g for 10 min at 37°C. Centrifugation of upper layer of the blood samples was performed again at 800g for 10 min in another tube. The supernatant containing the platelet-poor plasma was then removed. Finally, the left layer was PRP.

### Retinal microvascular endothelial cells proliferation assay

Retinal microvascular endothelial cells (RMECs) (the Cell Bank of the Chinese Academy of Sciences, Shanghai, China) were seeded on 96-well plates at a density of  $5 \times 10^3$  cells/well and cultured in DMEM-F12 (Biofluids, USA) at 37°C for 24 h. Cells were then stimulated with 0.1 mL PRP and 0.1 mL mock (10% FBS) respectively at 37°C for three days. Absorbance was measured at 450 nm with spectrophotometer (Thermo Scientific, Rockford, IL).

### Conjunction to DBM scaffolds

After dissolved in normal saline, CBD-BMP-2 was measured by ELISA. Anti-poly-histidine antibody (1:1000, Sigma, USA) was utilized as the primary antibody and alkaline phosphatase (ALP)-conjugated goat anti-mouse IgG (1:10,000 dilution, Sigma, USA) was selected as the secondary antibody. The procedures had been previously described.<sup>8,13</sup> DBMs were then respectively soaked in the CBD-BMP-2 solutions, PRP solutions, and the mixed solutions of CBD-BMP-2 and PRP at 37°C for 2 h. The concentrations of CBD-BMP-2 and PRP were 3 µg/DBM and 0.2 mL/DBM, respectively.

### Biological activity of CBD-BMP-2 and release assay in vitro

The procedures had been described in our previous study.<sup>8</sup> After cultured in DMEM-F12 (Biofluids, USA) for 24 h, the MC-3T3-E1 cells (the Cell Bank of the Chinese Academy of Sciences, Shanghai, China) were respectively stimulated

with CBD-BMP-2, commercial BMP-2 (East China Pharmaceutical Group Co. LTD, Hangzhou, China), and PRP for three days. Cells were then washed using PBS and lysed using 0.1% TritonX-100/PBS, followed by three times of freezing/thawing to disrupt cell membranes. Cell activities were presented as ALP activities that were determined with ALP reagent kit (ANASPEC, Fremont, CA, USA). DBM scaffolds respectively soaked CBD-BMP-2 and commercial BMP-2 was placed in different sterilized tubes containing 200  $\mu$ L PBS. At different time points (2 h, 4 h, 12 h, 24 h, 2d, and 3d), the scaffolds were removed from tubes and the released amount of protein in the tubes was determined with bicinchoninic acid protein assay reagent (Santa Cruz Biotechnology, USA).

### Surgical procedure

A minimally invasive operation with good reproducibility of posterolateral lumbar inter-transverse fusion was performed, which could reduce the mortality of these aging rats after surgery<sup>8,27</sup> (Figure 1). Three different fusion materials were implanted between left L4 and left L5 transverse processes. Rats implanted with the combination of DBM and CBD-BMP-2 + PRP were assigned to Group A ( $n=20$ ), implanted with DBM and CBD-BMP-2 were assigned to Group B ( $n=20$ ), and implanted with DBM and PRP were assigned to Group C ( $n=20$ ). Surgeries were completed by an experienced surgeon (S.L.). All rats were maintained in individual cages on a 12-h light-dark cycle at 22°C, fed with rat chow (1.24% calcium, 0.92% phosphorous), water, and antibiotics. After radiographic analysis, they were sacrificed for further study.

### Radiographic evaluation of spinal fusion

At four-week post-operation, radiographic assessment using posteroanterior radiograph scanner (Giotto image MD, Italy) was performed for each rat. On the radiographs, the presence of new formed bone connecting the two

transverse processes without any gap was considered as continuous bone bridge.<sup>28,29</sup>

Micro-computerized tomography ( $\mu$ CT) with high-resolution (SKYSCAN, Skyscan-1176, Belgium) was utilized to evaluate bone microstructure.<sup>8</sup> 3D images were reconstructed by CTVox software (Skyscan, Belgium). Mean fusion area at the cross-section view and total fusion volume on  $\mu$ CT images were calculated and then compared among the three groups. Mean area and total volume were calculated based on the cross-section view from the tip of transverse process of L4 to L5.

Bone microstructure was analyzed with CTAn software (Skyscan, Belgium) based on the  $\mu$ CT images.<sup>8</sup> Trabecular volume (TV), trabecular thickness (TT), and trabecular separation (TS) in a 1 mm<sup>3</sup> volume of interest (VOI) of fusion mass were calculated.<sup>30</sup> BMD referring to standard substances (Skyscan, Belgium) was also tested.<sup>31</sup> Two blinded independent authors (F.P. and X.S.) performed the radiographic analysis.

### Manual palpation

Spinal stability at the site of fusion was evaluated by manual palpation.<sup>8,32</sup> After the collection of spinal segments from L1 to sacrum, the two blinded independent authors (F.P. and X.S.) applied flexion and extension force on the intervertebral space between L4 and L5 of each sample. Motion was defined as mobility on both flexion and extension, partial motion was defined as mobility only on flexion or extension, and solid bony union was defined as no mobility neither on flexion nor on extension. Both motion and partial motion were recorded as non-solid bony union.

### Hematoxylin-eosin staining

Specimens near the grafting site were sectioned to a thickness of 20–25  $\mu$ m, followed by stained using hematoxylin and eosin (H&E). Stained sections were then examined

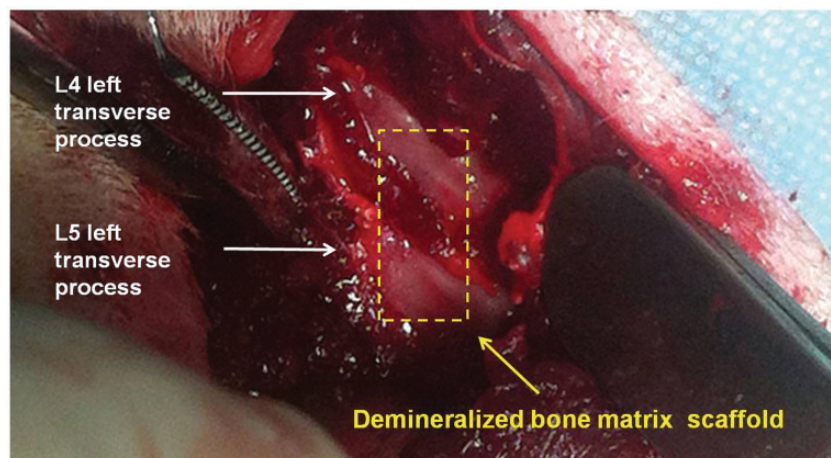


**Figure 1.** A 15–20 mm vertical midline incision in the skin and a left paramedian incision along the spinous processes through the dorsolumbar fascia was made. The left paravertebral muscles overlying the articular processes of L4–L5 were separated from the spinous processes by blunt dissection, followed by the exposure of left transverse processes of L4 and L5 (white arrow). After the transverse processes were decorticated with a high-speed burr until punctuate bleeding was observed, fusion materials were implanted (yellow arrow). In order to reduce the mortality caused by surgical trauma, only the left unilateral inter-transverse spinal fusion was performed. (A color version of this figure is available in the online journal.)

under fluorescence microscopy (Axio imager. M1, Zeiss, Germany).

### Statistical analysis

SPSS version 19.0 (Chicago, IL, USA) was used to perform statistical analysis. Data were presented as mean  $\pm$  standard deviation. Continuous data were compared among the three groups with ANOVA test. Categorical data were compared using nonparametric Chi-square test. *P* value  $<0.05$  was considered as statistically significant.

## Results

### The biological assays in vitro

After stimulation for three days, PRP was showed to be able to promote the proliferation of RMECs. The absorbance was  $0.453 \pm 0.046$  in the wells stimulated with PRP, while  $0.192 \pm 0.030$  in the wells with mock (10% FBS). In terms of osteogenesis, ALP activities in the wells stimulated with CBD-BMP-2 (3  $\mu\text{g}/\text{well}$ ) and commercial BMP-2 (3  $\mu\text{g}/\text{well}$ ) were both higher than that in the wells with PRP, while similar with each other. The release curves of CBD-BMP-2 and commercial BMP-2 are shown in Figure 2. Compared with commercial BMP-2, CBD-BMP-2 was obviously sustained released. After 12 h, releasing rate was significantly lower of CBD-BMP-2 than commercial BMP-2. At 48 h, almost all the commercial BMP-2 ( $90.4 \pm 6.6\%$ ) was released, while only  $18.7 \pm 7.2\%$  of CBD-BMP-2 was tested.

### Radiographic assessment of spinal fusion

Four weeks after implantation, two rats in Group A, two rats in Group B, and three rats in Group C died. All the other rats were performed radiographic assessment focusing on the efficiency of lumbar inter-transverse fusion. Evaluation based on plain radiographs observed 17 continuous bone bridges (94.4%) between L4 and L5 in Group A and 15 continuous bone bridges (83.3%) in Group B, while only 2 continuous bridges (11.8%) in Group C ( $P < 0.001$ , Figure 3).  $\mu\text{CT}$  images also presented better fusion efficiency in rats implanted with CBD-BMP-2 + PRP and CBD-BMP-2 than PRP, with larger fusion area at cross-section view and larger fusion mass on 3D reconstruction images (Figures 4 and 5(a, d and g)).

### Assessment of bone microarchitecture

The values of trabecular quantitative parameters are shown in Figure 5(b, e, f and h). TV of the new bone formation in a VOI of  $1 \text{ mm}^3$  was  $0.122 \pm 0.015 \text{ mm}^3$  in Group A,  $0.105 \pm 0.009 \text{ mm}^3$  in Group B, and  $0.062 \pm 0.003 \text{ mm}^3$  in Group C ( $P = 0.007$ ). TS was also significantly different among the three groups, with smaller value in Group A ( $P = 0.023$ ). TT was similar among the three groups. As a result, mean BMD of fusion mass in Group A was statistically larger than those in Groups B and C (Figure 5(c and i),  $P = 0.011$ ).

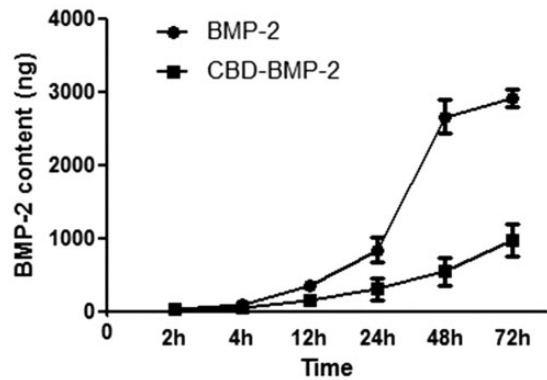


**Figure 2.** The release assay of CBD-BMP-2 *in vitro*. The releasing rate of CBD-BMP-2 was significantly lower than that of commercial BMP-2. At 48 h, only a few of CBD-BMP-2 was tested, while almost all the commercial BMP-2 was released.

### Manual palpation

After radiographic assessments, rats were sacrificed to collect lumbar specimens for manual palpation. Twenty-four rats were revealed to achieve solid lumbar fusion after surgery. The rate of solid bony union was 77.8% in Group A, 55.6% in Group B, and 0% in Group C (Table 1,  $P < 0.001$ ).

### Histological evaluation

H&E sections presented newly woven bone in the fusion mass in Groups A and B, with dense newly formed trabeculae surrounded by plentiful osteoblasts. Compared with Group C, there were more trabeculae and smaller trabecular separation in Groups A and B. Neither evidence of foreign body rejection nor reaction such as inflammation or debris encapsulation was found (Figure 6).

## Discussion

Osteoporosis leading to delayed bone healing, nonunion, and increased postoperative complications has pushed researchers to investigate efficient biomaterial for reinforcing bone fusion in animal models. After approved for clinical application by the US Food and Drug Administration, BMP-2 has been widely used as an alternative bone graft in spinal fusion procedures.<sup>33,34</sup> With the aim of alleviating systemic adverse effects associated with the burst release and supraphysiological dosage of BMP-2, various targeted therapies have been developed including the genetically engineered CBD-BMP-2. Previous studies have demonstrated the similar biological activity of CBD-BMP-2 with natural BMP-2 and its sustained releasing ability in a prolonged time.<sup>8,14-16</sup> Adult<sup>15</sup> and infant<sup>16</sup> animal models both supported that the local highly concentrated CBD-BMP-2 could promote bone regeneration and meanwhile diminish the adverse effects.

Sustained releasing and prolonged osteogenetic effect would have more values in senile subjects who were often complained with decreased spinal fusion rate. Up to now, however, this effective targeted therapy has not been investigated in the aging body. Due to having similar bone metabolisms with human, rats provide invaluable insights

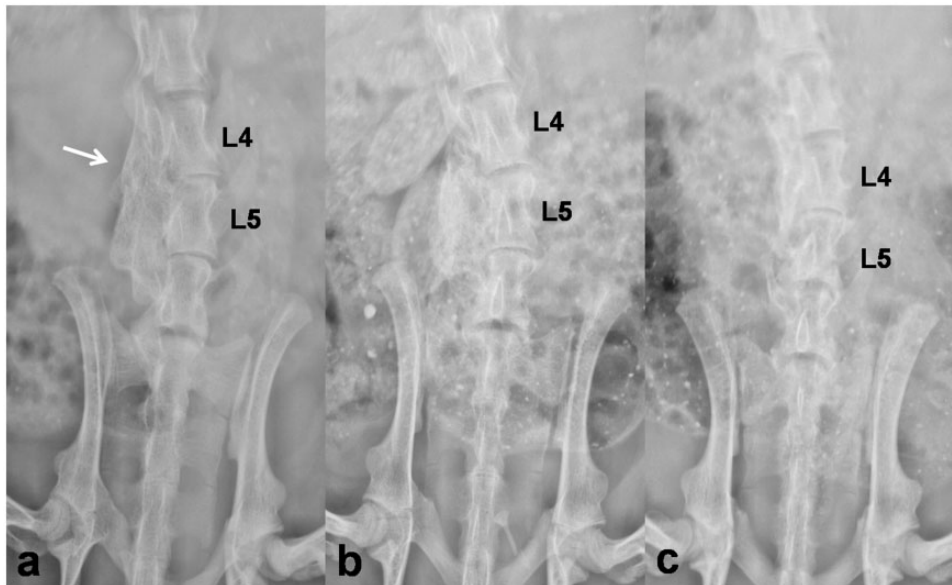


**Figure 3.** Plain radiographs (coronal view) of lumbar at four weeks after implantation. Obvious bone bridges were detected between the left transverse processes of L4 and L5 in the 18 rats implanted with CBD-BMP2 + PRP (a) and in the 18 rats implanted with CBD-BMP2 (b). Continuous bone bridges were not observed in the 17 rats implanted with PRP (c). The white arrow indicates implant site.

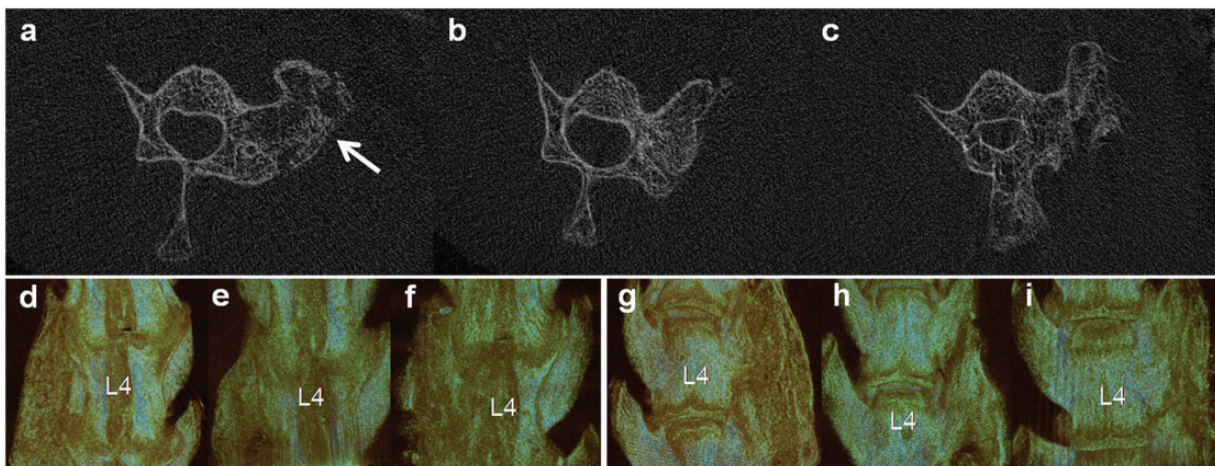


**Figure 4.**  $\mu$ CT assessment of the fusion mass at four weeks after implantation (a, b, c Cross-section views, d-i 3D reconstructions). In the cross-section view, more new bone formation was induced in the 18 rats implanted with CBD-BMP2 + PRP (a) and the 18 rats with CBD-BMP2 (b) than the 17 rats with PRP (c). The white arrow indicates implant site. In 3D reconstructions images (d, e, f dorsal view, g, h, i ventral view), continuous and considerable fusion mass was only observed in rats implanted with CBD-BMP2 + PRP (d, g). In rats implanted with CBD-BMP2 (e, h), the fusion mass was relatively smaller than those with CBD-BMP2 + PRP (d, g). In rats implanted with PRP (e, h), the new bone formation was scattered, which was not merged into a whole mass. (A color version of this figure is available in the online journal.)

to our understanding of bone biology, bone decay mechanism, and osteoporosis-related malunion. However, most authors performed their studies in young models whose osteopenia was induced by physical or chemical methods.<sup>35,36</sup> It is not reasonable to perform a study concerning an age-related disease in young body, whose physiological function, metabolic rate, and bone microenvironment are quite different from the aging body.

In order to simulate the physiological condition of aging body, senile rats aged 18 months that were equivalent to the aged stage of normal people were selected as the experimental subjects in the present study.<sup>24</sup> Osteopenia was identified by dual-energy X-ray

absorptiometry. Despite the dysfunction of bone cells in aging body, osteoinduction could still be activated in response to the stimulation of BMP-2. *In vivo* experiments showed satisfactory efficiency of lumbar inter-transverse fusion with acceptable radiographic and histological assessments (Table 1, Figures 3 to 6). The measurable different results reminded that general osteogenic management might not be equally applicable to the elderly. Compared with the results in young healthy rats,<sup>8</sup> TV ( $0.142 \pm 0.014 \text{ mm}^3$  vs.  $0.105 \pm 0.009 \text{ mm}^3$ ), BMD ( $0.496 \pm 0.106 \text{ mg/mm}^3$  vs.  $0.284 \pm 0.047 \text{ mg/mm}^3$ ), and solid fusion rate (95% vs. 66.7%) were relatively smaller in the current study. In our opinions, the osteogenetic dysfunction

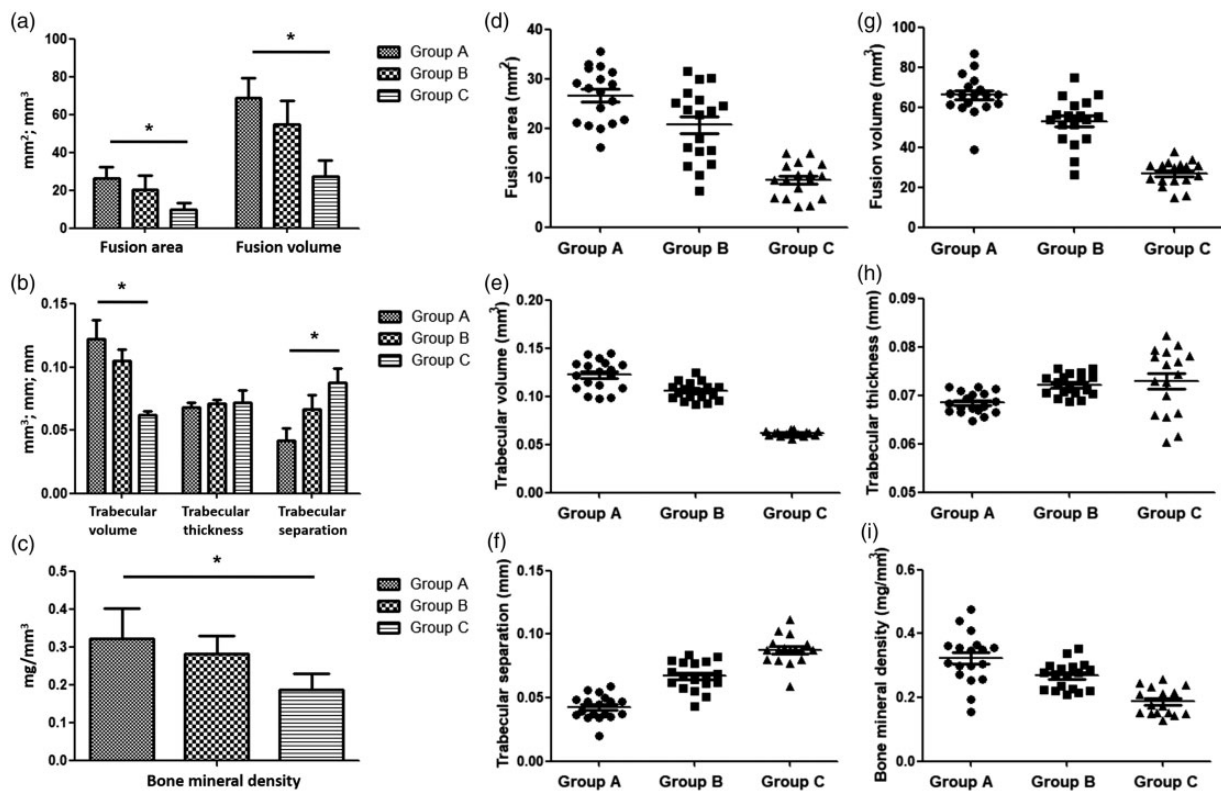


**Figure 5.** Assessment of the new bone formation by  $\mu$ CT. (a) Mean fusion area (FA) in cross-section view and total fusion volume (FV) in 3D reconstruction of new bone formation were greater in Group A including 18 survived rats than Group B including 18 rats and Group C with 17 rats. (b) Compared with Groups B and C, Group A had the larger trabecular volume (TV) and smaller trabecular separation (TS). Trabecular thickness (TT) was similar among the three groups. (c) Bone mineral density was larger in Group A than the other two groups. Statistical significance was  $*P < 0.05$ . (d-i) The data were presented as dot plots.

**Table 1.** Manual palpation evaluation.

	N	Group			$P^*$
		Group A (n = 18)	Group B (n = 18)	Group C (n = 17)	
Motion	11	0	1	10	<0.001
Partial motion	16	4	5	7	0.457
No motion	26	14	12	0	<0.001
N	53	18	18	17	

\*Calculated by Chi-square analysis.

and aging condition in osteopenia rats should be both responsible for the inferior outcome.

The bone repair was a complicated process that included stem cell differentiation, osteogenesis, and angiogenesis. In recent years, bone microcirculatory disturbance was increasingly considered as one of the pathogenesis of age-related osteoporosis.<sup>17-19</sup> We believed facilitating osteogenesis by one aspect might not be enough to achieve an inspiring result, especially for the aging body. Containing various osteogenic and angiogenic growth factors, PRP was also used to accelerate bone healing.<sup>37,38</sup> *In vitro* assay in the present study showed PRP was effective in promoting the proliferation of RMECs, but animal models did not present satisfactory efficiency of fusion when rats implanted with PRP alone (Table 1, Figures 3 to 6). Based on the physiological characteristics of both osteogenetic and angiogenic dysfunction in aging body, we transplanted the combination of

CBD-BMP-2 and PRP in senile rat models with osteopenia. Four weeks after implantation, the radiographic assessments revealed better efficiency with larger fusion area, larger fusion volume, more trabeculae, and greater BMD in Group A than Groups B and C (Table 1, Figures 3 to 6); 77.8% of rats in Group A reached solid fusion, while 66.7% in Group B and no rat in Group C reached solid bony union. In addition, histological assessment was also better in Group A when compared with Groups B and C. We thought the ambidextrous promotions on the osteogenesis and angiogenesis were responsible for this desirable efficiency.

Selecting aging body as subjects embraced all the age-related risk factors of osteopenia. The optimistic results in the current study indicated that CBD-BMP-2 combined with PRP was an enhanced bioactive osteogenetic management for senile osteopenia rats. In addition, BMP-2 and PRP have the advantages of large quantity, easy availability, and

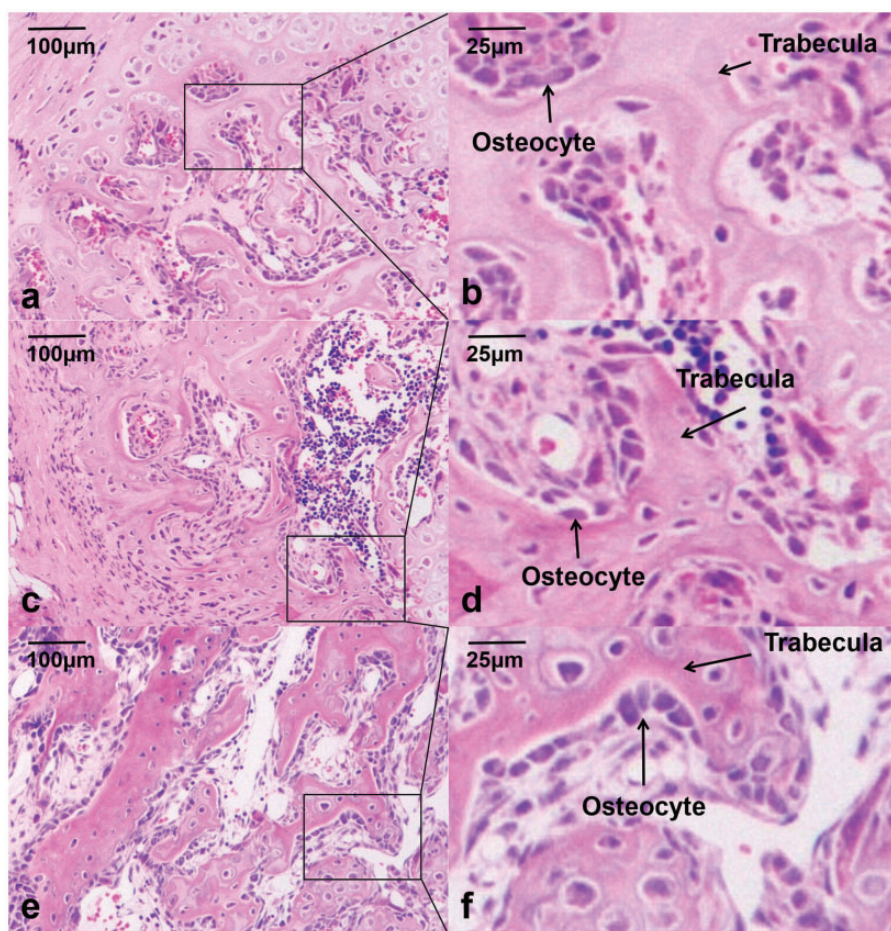


**Figure 6.** Histological observations using hematoxylin–eosin staining. The staining showed more osteocytes, more trabeculae, and smaller trabecular separation in the 18 rats implanted with CBD-BMP2 + PRP (a, b) and the 18 rats CBD-BMP2 (c, d) than the 17 rats with PRP (e, f). (A color version of this figure is available in the online journal.)

better biocompatibility, giving this osteogenic strategy a promising prospect of application and spreading. Despite the above findings, some limitations should be addressed. First, we did not directly evaluate the microvessel repair function of PRP. Second, X-ray analysis, manual palpation, and histological evaluation were to some extent subjective, which was remedied by the quantitative parameters in  $\mu$ CT evaluation. Third, the duration of biological materials implanted in rats was relatively short. With the consideration of more aged rats might die after surgery, we did not prolong the implanted time. It would be better to perform the radiographic and histological assessment over longer time after implantation, which would strengthen the reliability of results. Fourth, bone formation and resorption biomarkers were not tested in the present study, which could help better explaining the mechanisms of promoting bone defect healing by the implanted materials. Fifth, we only performed investigation in male rats. Further investigations are warranted in female rats. In addition, sham controls that are only implanted DBM or implanted nothing should also be included. Finally, large animals could provide more proper vertebral defects with biomechanics analysis.

In summary, the current study determined that DBM-CBD-BMP-2 could effectively facilitate the lumbar inter-transverse fusion in aged rats with osteopenia. PRP could help DBM-CBD-BMP-2 to enhance the bone healing of vertebral defects with better radiographic and histological results. DBM, BMP-2, and PRP have the advantages of large quantity, easy availability, and better biocompatibility, enabling this bone repair system more practicable and promising for clinical application in aging body.

#### AUTHORS' CONTRIBUTIONS

ZWG contributed to the study design and drafted the manuscript. LSB performed the surgeries and participated in the design of the study. KC and PFM collected and analyzed the data. OYM and SK reviewed and edited the manuscript. All authors read and approved the final manuscript.

#### DECLARATION OF CONFLICTING INTERESTS

The author(s) declared no potential conflicts of interest with respect to the research, authorship, and/or publication of this article.

## FUNDING

The author(s) disclosed receipt of the following financial support for the research, authorship, and/or publication of this article: This work was funded by China Postdoctoral Science Foundation and Beijing Postdoctoral Research Foundation.

## ORCID iD

Weiguo Zhu  <https://orcid.org/0000-0002-7451-9062>

## REFERENCES

- Rometsch E, Spruit M, Zigler JE, Menon VK, Ouellet JA, Mazel C, Härtl R, Espinoza K, Kandziora F. Screw-related complications after instrumentation of the osteoporotic spine: a systematic literature review with meta-analysis. *Global Spine J* 2020;**10**:69–88
- Bjerke BT, Zarrabian M, Aleem IS, Fogelson JL, Currier BL, Freedman BA, Bydon M, Nassr A. Incidence of osteoporosis-related complications following posterior lumbar fusion. *Global Spine J* 2018;**8**:563–9
- Marie PJ, Kassem M. Osteoblasts in osteoporosis: past, emerging, and future anabolic targets. *Eur J Endocrinol* 2011;**165**:1–10
- Kanakaris NK, Tzioupis C, Nikolaou VS, Papatheanasopoulos A, Giannoudis PV. The influence of osteoporosis in femoral fracture healing time. *Injury* 2009;**40**:663–8
- Tarantino U, Cerocchi I, Scialdoni A, Saturnino L, Feola M, Celi M, Liuni FM, Iolascon G, Gasbarra E. Bone healing and osteoporosis. *Aging Clin Exp Res* 2011;**23**:62–4
- Makino T, Tsukazaki H, Ukon Y, Tateiwa D, Yoshikawa H, Kaito T. The biological enhancement of spinal fusion for spinal degenerative disease. *Int J Mol Sci* 2018;**19**:2430
- Chao L, Songlin P, Jie L, Jun L, Daogang G, Feng J, Cheng L, Fangfei L, Xiaojuan H, Hailong Z, Dazhi Y, Bao-Ting Z, Aiping L, Ge Z, Au DWT. Inhibition of osteoblastic Smurf1 promotes bone formation in mouse models of distinctive age-related osteoporosis. *Nat Commun* 2018;**9**:3428
- Zhu W, Qiu Y, Sheng F, Yuan X, Xu L, Bao H, Dai J, Zhu Z. An effective delivery vehicle of demineralized bone matrix incorporated with engineered collagen-binding human bone morphogenetic protein-2 to accelerate spinal fusion at low dose. *J Mater Sci Mater Med* 2017;**29**:2
- P, Haubruck M, Tanner W, Vlachopoulos S, Hagelskamp M. Comparison of the clinical effectiveness of bone morphogenetic protein (BMP) -2 and -7 in the adjunct treatment of lower limb nonunions. *Orthop Traumatol Surg Res* 2018;**104**:1241–8
- Lee SS, Huang BJ, Kaltz SR, Sur S, Newcomb CJ. Bone regeneration with low dose BMP-2 amplified by biomimetic supramolecular nanofibers within collagen scaffolds. *Biomaterials* 2013;**34**:452–9
- Faundez A, Tournier C, Garcia M, Aunoble S, Le Huec J-C. Bone morphogenetic protein use in spine surgery – complications and outcomes: a systematic review. *Int Orthop* 2010;**40**:1309–19
- Chen B, Lin H, Zhao Y, Wang B, Zhao Y, Liu Y, Liu Z, Dai J. Activation of demineralized bone matrix by genetically engineered human bone morphogenetic protein-2 with a collagen binding domain derived from von willebrand factor propolypeptide. *J Biomed Mater Res A* 2007;**80**:428–34
- Chen B, Lin H, Wang J, Zhao Y, Wang B, Zhao W, Sun W, Dai J. Homogeneous osteogenesis and bone regeneration by demineralized bone matrix loading with collagen-targeting bone morphogenetic protein-2. *Biomaterials* 2007;**28**:1027–35
- Zhao Y, Chen B, Lin H, Sun W, Zhao W, Zhang J, Dai J. The bone-derived collagen containing mineralized matrix for the loading of collagen-binding bone morphogenetic protein-2. *J Biomed Mater Res A* 2009;**88**:725–34
- Han X, Zhang W, Gu J, Zhao H, Ni L, Han J, Zhou Y, Gu Y, Zhu X, Sun J, Hou X, Yang H, Dai J, Shi Q. Accelerated postero-lateral spinal fusion by collagen scaffolds modified with engineered collagen-binding human bone morphogenetic protein-2 in rats. *PLoS One* 2014;**9**:e98480
- Cui Y, Xu B, Yin Y, Chen B, Zhao Y, Xiao Z, Yang B, Shi Y, Fang Y, Ma X, Dai J. Collagen particles with collagen-binding bone morphogenetic protein-2 promote vertebral laminar regeneration in infant rabbits. *Biomed Mater* 2020;**15**:055008
- Liu Y, Cao L, Hillengass J, Delorme S, Schlewitz G, Govindarajan P, Schnettler R, Heiss C, Bauerle T. Quantitative assessment of microcirculation and diffusion in the bone marrow of osteoporotic rats using VCT, DCE-MRI, DW-MRI, and histology. *Acta Radiol* 2013;**54**:205–13
- Sun MH, Leung K-S, Zheng Y-P, Huang Y-P, Wang L-K, Qin L, Leung AH-C, Chow SK-H, Cheung W-H. Three-dimensional high frequency power Doppler ultrasonography for the assessment of microvasculature during fracture healing in a rat model. *J Orthop Res* 2012;**30**:137–43
- Ding W-G, Wei Z-X, Liu J-B. Reduced local blood supply to the tibial metaphysis is associated with ovariectomy-induced osteoporosis in mice. *Connect Tissue Res* 2011;**52**:25–9
- Ramasamy SK, Kusumbe AP, Schiller M, Zeuschner D, Bixel MG, Milia C, Gamrekelashvili J, Limbourg A, Medvinsky A, Santoro MM, Limbourg FP, Adams RH. Blood flow controls bone vascular function and osteogenesis. *Nat Commun* 2016;**7**:13601
- Ou-Yang L, Guang-Ming L. Dysfunctional microcirculation of the lumbar vertebral marrow prior to the bone loss and intervertebral disc degeneration. *Spine* 2015;**40**:E593–600
- Myung H, Jang H, Myung JK, Lee C, Lee J, Kang JH, Jang WS, Lee SJ, Kim H, Kim HY, Park S, Shim S. Platelet-rich plasma improves the therapeutic efficacy of mesenchymal stem cells by enhancing their secretion of angiogenic factors in a combined radiation and wound injury model. *Exp Dermatol* 2020;**29**:158–67
- Kim ES, Kim JJ, Park EJ. Angiogenic factor-enriched platelet-rich plasma enhances in vivo bone formation around alloplastic graft material. *J Adv Prosthodont* 2010;**2**:7–13
- Zeng JH, Zhong ZM, Li XD, Wu Q, Zheng S, Zhou J, Ye WB, Xie F, Wu XH, Huang ZP, Chen JT. Advanced oxidation protein products accelerate bone deterioration in aged rats. *Exp Gerontol* 2014;**50**:64–71
- Schouten CC, Hartman EH, Spauwen PH, Jansen JA. DBM induced ectopic bone formation in the rat: the importance of surface area. *J Mater Sci Mater Med* 2005;**16**:149–52
- Farzaneh D, Narges S, Hossein B, MRP, Saied K-D. The use of platelet-rich plasma (PRP) to improve structural impairment of rat testis induced by busulfan. *Platelets* 2019;**30**:513–20
- Bobyn J, Rasch A, Little DG, Schindeler A. Posterolateral intertransverse lumbar fusion in a mouse model. *J Orthop Surg Res* 2013;**8**:2
- Kong CB, Lee JH, Baek HR, Lee CK, Chang BS. Posterolateral lumbar fusion using *Escherichia coli*-derived rhBMP-2/hydroxyapatite in the mini pig. *Spine J* 2014;**14**:2959–67
- Zhao H, Guan HG, Gu J, Luo ZP, Zhang W, Chen B, Gu QL, Yang HL, Shi Q. Collagen membrane alleviates peritendinous adhesion in the rat achilles tendon injury model. *Chin Med J* 2013;**126**:729–33
- Bouxsein ML, Boyd SK, Christiansen BA, Guldberg RE, Jepsen KJ, Muller R. Guidelines for assessment of bone microstructure in rodents using micro-computed tomography. *J Bone Miner Res* 2010;**25**:1468–86
- Miyazaki M, Morishita Y, He W, Hu M, Sintuu C, Hymanson HJ, Falakassa J, Tsumura H, Wang JC. A porcine collagen-derived matrix as a carrier for recombinant human bone morphogenetic protein-2 enhances spinal fusion in rats. *Spine J* 2009;**9**:22–30
- Hsu HP, Zanella JM, Peckham SM, Spector M. Comparing ectopic bone growth induced by rhBMP-2 on an absorbable collagen sponge in rat and rabbit models. *J Orthop Res* 2006;**24**:1660–9
- Sandhu HS, Khan SN. Recombinant human bone morphogenetic protein-2: use in spinal fusion applications. *J Bone Joint Surg Am* 2003;**85-A**:89–95
- Deyo RA, Ching A, Matsen L, Martin BI, Kreuter W, Jarvik JG, Angier H, Mirza SK. Use of bone morphogenetic proteins in spinal fusion surgery for older adults with lumbar stenosis: trends, complications, repeat surgery, and charges. *Spine* 2012;**37**:222–30
- Ghodasra J, Nickoli M, Hashmi S, Nelson J, Mendoza M, Nicolas J, Bellary S, Sonn K, Ashtekar A, Park C. Ovariectomy-induced osteoporosis does not impact fusion rates in a recombinant human bone



- morphogenetic protein-2-dependent rat posterolateral arthrodesis model. *Global Spine J* 2016;**06**:60-8
36. Zhang Z, Hui R, Shen G, Qiu T, Wei Q. Animal models for glucocorticoid-induced postmenopausal osteoporosis: an updated review. *Biomed Pharmacother* 2016;**84**:438-46
37. Butterfield KJ, Bennett J, Gronowicz G, Adams D. Effect of platelet-rich plasma with autogenous bone graft for maxillary sinus augmentation in a rabbit model. *J Oral Maxillofac Surg* 2005;**63**:370-7
38. Zhou D, Tian B, Feng L, Zeng W, Chang W. Bone regeneration combining platelet rich plasma with engineered bone tissue. *J Biomater Tissue Eng* 2017;**7**:841-7

(Received November 17, 2020, Accepted February 17, 2021)